CHEMISTRY OF MATERIALS

Communication

pubs.acs.org/cm

Synthesis and Electrical Properties of Covalent Organic Frameworks with Heavy Chalcogens

Selma Duhović and Mircea Dincă*

Department of Chemistry, Massachusetts Institute of Technology, Cambridge, Massachusetts 02139, United States

Supporting Information

Significant research has been devoted to capturing the Sun's energy with both inorganic and organic materials. Although the challenges are myriad, transformative discoveries in the latter class fall squarely in the realm of synthetic chemistry. Despite being lightweight, mechanically flexible, as well as easily and affordably processed, organic photovoltaics suffer from lower efficiencies and lifetimes than commercial inorganic solar cells. Such limitations stem both from morphological defects and from weak electronic coupling coupled to strong electron−phonon interactions. These work together to affect exciton formation, migration, and dissociation, as well as charge transfer and separation at the electrodes.[1−5] Controlling the way donor and acceptor moieties are assembled is thus key to improving the performance of photovoltaics and other organic electronic devices.[6]

One class of materials that can address this challenge is covalent organic frameworks (COFs),[7−28] whose periodicity, dimensionality, and rigidity allow for optimization of molecular architecture and of intra- and intermolecular interactions. Although the majority of COFs lack significant bulk electrical conductivity, their potential to harvest light and conduct electricity is beginning to be tapped.[29−32] Most relevantly, Jin et al. explored charge dynamics in donor−acceptor COFs and showed that the inherent bicontinuous heterojunction allows direct coupling of light absorption, exciton generation, and charge separation.[16] In 2013, chalcogenophene-based COFs were reported with the use of thiophene, dithiophene, and thienothiophene diboronic acids. These materials engage in unique charge-transfer interactions with electron acceptors such as TCNQ,[33] a first requirement for developing charge and exciton-diffusion materials, and can be used as active materials for organic photovoltaic devices.[34] Even more recently, reports on COFs based on benzodithiophene[35] and tetrathiafulvalene[36−38] were published.

Here, we report our efforts to leverage the structural features of COFs and introduce the first heavier chalcogen-based materials in the form of fused benzodiselenophenes and benzoditellurophenes. The motivation behind the design of chalcogenophene-containing fused-aromatic COFs stems from the leading role of fused chalcogenophenes in organic conductors, narrow band gap polymers, and field-effect transistors.[39−43] Use of heavy chalcogen atoms has been shown to increase charge mobility in organic photovoltaic materials, presumably through the enhanced orbital overlap afforded by the 3p and 4p orbitals of selenium and tellurium atoms, respectively, or through enhanced spin−orbit coupling effects.[44−46] Indeed, whereas thiophene-based polymers have larger optical band gaps (1.9 eV in polythiophene vs. 1.5 eV in CdTe[47]) and much smaller charge mobility values than inorganic semiconductors(0.1 $cm^2\ V^{-1}\ s$ in polythiophene vs. 100−1000 $cm^2\ V^{-1}\ s$ in indium zinc oxide[48]), replacing sulfur with selenium reduces the optical band gap to 1.6 eV.[49−51] The close stacking of selenium and tellurium is also expected to reduce the impact of disorder in the self-assembly process required for COF synthesis and generate more disperse bands to enhance interchain packing of the framework. This should lead to increased conductivity for the heavier chalcogen materials without significantly changing the structure or the unit cell size of the resulting extended networks.[52] Herein, we report the synthesis and characterization of the first COFs that incorporate selenium and tellurium atoms into the backbone and show that the presence of the heavier chalcogens indeed leads to superior electrical properties relative to the thiophene analogue.

Treatment of trimethylsilyl-protected benzo[1,2-b:4,5-b′]-diselenophene and benzo[1,2-b:4,5-b′]ditellurophene[53] with BBr_3, followed by basic hydrolysis and subsequent acidification afforded the new diboronic acids benzo[1,2-b:4,5-b′]-diselenophene (**H_2BDSe**) and benzo[1,2-b:4,5-b′]-ditellurophene (**H_2BDTe**) in good yields (Scheme 1). For comparison purposes, we also synthesized the reported benzodithiophene analogue (**H_2BDS**).[35] All three benzodichalcogenophene diboronic acids were fully characterized using standard methods.

Scheme 1. Synthesis of Benzodichalcogenophene Diboronic Acid Precursors

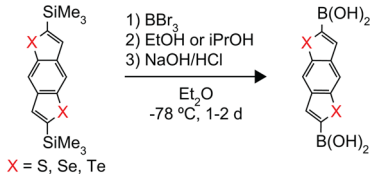

Condensation of the diboronic acids with 2,3,6,7,10,11-hexahydroxytriphenylene (**HHTP**) in a 1:1 mixture of mesitylene and 1,4-dioxane led to the isolation of green crystalline powders after heating at 120 °C for 24−72 h (Scheme 2). After washing with fresh 1,4-dioxane and dichloromethane, then drying under reduced pressure for 12 h, these powders were formulated as $(HOTP)_2(BDT)_3$ (**1-S**;

Received: June 22, 2015
Revised: July 30, 2015
Published: July 30, 2015

DOI: 10.1021/acs.chemmater.5b02358
Chem. Mater. 2015, 27, 5487−5490

Scheme 2. Synthesis of 1-S, 1-Se, and 1-Te

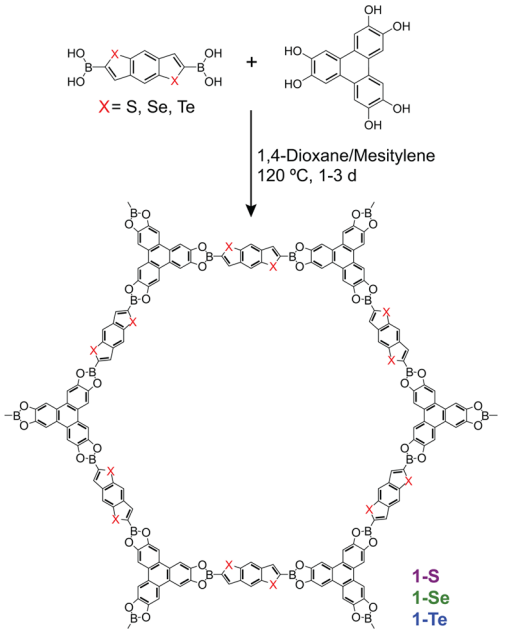

HOTP = 2,3,6,7,10,11-hexaoxytriphenylene, BDT = benzodithiophene diboronate), $(HOTP)_2(BDSe)_3$ (**1-Se**; BDSe = benzodiselenophene diboronate), and $(HOTP)_2(BDTe)_3$ (**1-Te**; BDTe = benzoditellurophene diboronate) and verified by C, H, and N elemental analyses.

Powder X-ray diffraction (PXRD) patterns of each of these materials (Figure 1) exhibited peaks indicative of the formation of hexagonal 2D layers stacked in an eclipsed manner, with unit cell lengths, $a = b = 36.5$ and 36.7 Å, and interlayer distance, $c =$ 3.40 and 3.45 Å for **1-Se** and **1-Te**, respectively.

Strong bands observed at 1398, 1395, and 1383 cm^{-1} (Figure 2) in the infrared (IR) spectra of **1-S**, **1-Se**, and **1-Te**, respectively, attributed to the asymmetric B−O stretches, confirmed the formation of boronate ester links.[54] Furthermore, for all three COFs, characteristic bands corresponding to C−B stretches in the chalcogenophene and C−O stretches in the catechol moieties were observed at approximately 1062 and 1241 cm^{-1}, respectively. Thermogravimetric analyses (TGA) (Figures S26−S28) revealed the most drastic weight loss to be at ∼380 °C for **1-S** and 440−500 °C for **1-Se** and **1-Te**. The weight loss at lower temperatures is attributed to evaporation of dioxane (b.p. 101 °C) and mesitylene (b.p. 160 °C) guest molecules.

After degassing at 200 °C for 24 h at 2 mTorr, samples of **1-S** and **1-Se** adsorbed 701 and 672 cm^3 of N_2 gas per gram, respectively, at 77 K and 760 Torr (Figure 3). Fitting the P/P_0

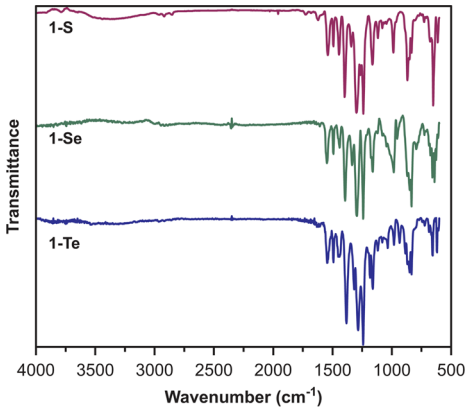

Figure 2. IR spectra of **1-S**, **1-Se**, and **1-Te**.

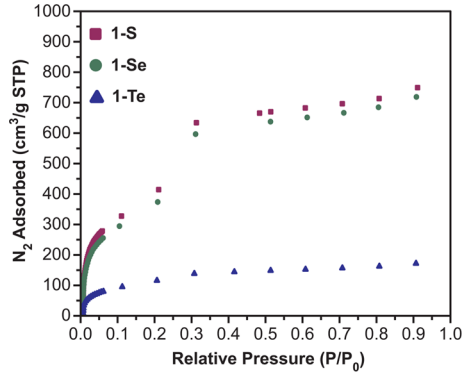

Figure 3. Nitrogen adsorption isotherms for **1-S**, **1-Se**, and **1-Te** at 77 K.

$\lesssim 0.2$ region of the N_2 adsorption isotherms to the BET model revealed surface areas of 1125 m^2/g (1424 $m^2/mmol$) and 1056 m^2/g (1634 $m^2/mmol$), for **1-S** and **1-Se**, respectively. Measurements of two different sample batches of **1-Te**, activated under similar conditions, led to uptakes of only 148−164 cm^3 of N_2 per gram, which corresponds to a BET surface area of 302−352 m^2/g (555−647 $m^2/mmol$). Unlike **1-S** and **1-Se**, **1-Te** becomes less crystalline upon activation (Figure S27). Activation at 150 °C showed no improvement in surface area measurements. Although it is unclear what causes the difference in N_2 uptake between these compounds, possible explanations include the somewhat lower crystallinity of **1-Te** and potential surface pore blocking effects.[55]

Despite its lower crystallinity, which likely leads to an increase in overall resistance because of grain boundaries, **1-Te** exhibits the highest bulk conductivity of the three COFs. Indeed, two-point probe electrical conductivity measurements of compressed pellets of these materials revealed values of

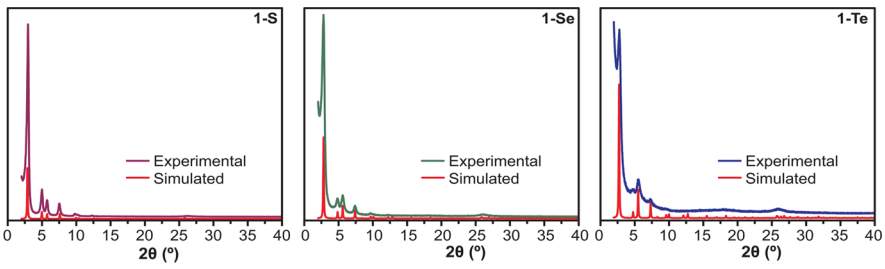

Figure 1. Experimental and simulated PXRD patterns of **1-S**, **1-Se**, and **1-Te**.

DOI: 10.1021/acs.chemmater.5b02358
Chem. Mater. 2015, 27, 5487−5490

3.7(±0.4) × 10^{-10} S/cm for **1-S**, 8.4(±3.8) × 10^{-9} S/cm for **1-Se**, and 1.3(±0.1) × 10^{-7} S/cm for **1-Te** (Figure 4). Notably,

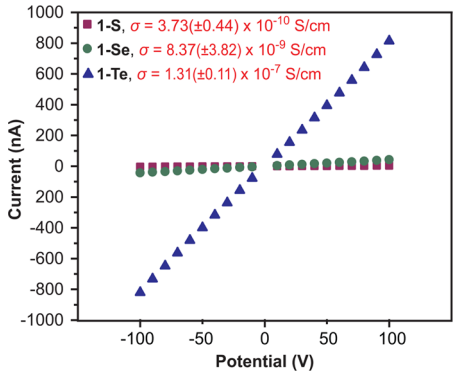

Figure 4. Current−voltage curves of pressed pellets of undoped **1-S**, **1-Se**, and **1-Te** at ambient temperature.

all three COFs show conductivities that are higher than those of the diboronic acid precursors (σ = 8.0(±1.7) × 10^{-13} S/cm for **H_2BDS**; σ = 1.2(±0.2) × 10^{-10} S/cm for **H_2BDSe**; σ = 6.2(±2.6) × 10^{-9} S/cm for **H_2BDTe**). However, the conductivity of the **HHTP** precursor itself was 2.5(±0.1) × 10^{-8} S/cm.

Although the increase in going from the diboronic acid precursors to the COFs may be due to the addition of HHTP, especially in an ordered π-stacked fashion, this suggests that the conductivity increase in the order S < Se < Te in both the precursors and COFs is indeed due to the presence of increasingly larger chalcogens.

The foregoing results highlight the utility of the heavier chalcogens for improving the charge transport properties of COFs. The first examples of COFs based on selenium and tellurium should provide a blueprint for similar studies in this burgeoning area. Our efforts are now focused on engineering thin films of these materials for use in solar cell and field-effect transistors.

■ ASSOCIATED CONTENT

Supporting Information

The Supporting Information is available free of charge on the ACS Publications website at DOI: 10.1021/acs.chemmater.5b02358.

Experimental details, NMR, PXRD, IR, TGA, UV−Vis, adsorption isotherms, *I*−*V* curves (PDF)

■ AUTHOR INFORMATION

Corresponding Author

*E-mail: mdinca@mit.edu.

Notes

The authors declare no competing financial interest.

■ ACKNOWLEDGMENTS

This work was supported by the U.S. Department of Energy, Office of Science, Office of Basic Energy Sciences (U.S. DOE-BES) under award no. DE-SC0006937. MD thanks the Sloan Foundation, the Research Corporation for Science Advancement (Cottrell Scholar program), and 3M for nontenured faculty awards.

■ REFERENCES

(1) Menke, S. M.; Holmes, R. J. Exciton Diffusion in Organic Photovoltaic Cells. *Energy Environ. Sci.* **2014**, *7*, 499−512.
(2) Clarke, T. M.; Durrant, J. R. Charge Photogeneration in Organic Solar Cells. *Chem. Rev.* **2010**, *110*, 6736−6767.
(3) Liang, Y.; Yu, L. Development of Semiconducting Polymers for Solar Energy Harvesting. *Polym. Rev.* **2010**, *50*, 454−473.
(4) Guo, X.; Baumgarten, M.; Müllen, K. Designing π-Conjugated Polymers for Organic Electronics. *Prog. Polym. Sci.* **2013**, *38*, 1832−1908.
(5) Chochos, C. L.; Choulis, S. A. How the Structural Deviations on the Backbone of Conjugated Polymers Influence Their Optoelectronic Properties and Photovoltaic Performance. *Prog. Polym. Sci.* **2011**, *36*, 1326−1414.
(6) Loos, J. Volume Morphology of Printable Solar Cells. *Mater. Today* **2010**, *13*, 14−20.
(7) Koo, B. T.; Dichtel, W. R.; Clancy, P. A Classification Scheme for the Stacking of Two-Dimensional Boronate Ester-Linked Covalent Organic Frameworks. *J. Mater. Chem.* **2012**, *22*, 17460−17469.
(8) Spitler, E. L.; Koo, B. T.; Novotney, J. L.; Colson, J. W.; Uribe-Romo, F. J.; Gutierrez, G. D.; Clancy, P.; Dichtel, W. R. A 2D Covalent Organic Framework with 4.7-nm Pores and Insight into Its Interlayer Stacking. *J. Am. Chem. Soc.* **2011**, *133*, 19416−19421.
(9) Colson, J. W.; Dichtel, W. R. Rationally Synthesized Two-Dimensional Polymers. *Nat. Chem.* **2013**, *5*, 453−465.
(10) Brucks, S. D.; Bunck, D. N.; Dichtel, W. R. Functionalization of 3D Covalent Organic Frameworks Using Monofunctional Boronic Acids. *Polymer* **2014**, *55*, 330−334.
(11) Spitler, E. L.; Colson, J. W.; Uribe-Romo, F. J.; Woll, A. R.; Giovino, M. R.; Saldivar, A.; Dichtel, W. R. Lattice Expansion of Highly Oriented 2D Phthalocyanine Covalent Organic Framework Films. *Angew. Chem., Int. Ed.* **2012**, *51*, 2623−2627.
(12) Colson, J. W.; Woll, A. R.; Mukherjee, A.; Levendorf, M. P.; Spitler, E. L.; Shields, V. B.; Spencer, M. G.; Park, J.; Dichtel, W. R. Oriented 2D Covalent Organic Framework Thin Films on Single-Layer Graphene. *Science* **2011**, *332*, 228−231.
(13) Feng, X.; Chen, L.; Honsho, Y.; Saengsawang, O.; Liu, L.; Wang, L.; Saeki, A.; Irle, S.; Seki, S.; Dong, Y.; et al. An Ambipolar Conducting Covalent Organic Framework with Self-Sorted and Periodic Electron Donor-Acceptor Ordering. *Adv. Mater.* **2012**, *24*, 3026−3031.
(14) Feng, X.; Chen, L.; Dong, Y.; Jiang, D. Porphyrin-Based Two-Dimensional Covalent Organic Frameworks: Synchronized Synthetic Control of Macroscopic Structures and Pore Parameters. *Chem. Commun.* **2011**, *47*, 1979−1981.
(15) Nagai, A.; Chen, X.; Feng, X.; Ding, X.; Guo, Z.; Jiang, D. A Squaraine-Linked Mesoporous Covalent Organic Framework. *Angew. Chem., Int. Ed.* **2013**, *52*, 3770−3774.
(16) Jin, S.; Furukawa, K.; Addicoat, M.; Chen, L.; Takahashi, S.; Irle, S.; Nakamura, T.; Jiang, D. Large Pore Donor-Acceptor Covalent Organic Frameworks. *Chem. Sci.* **2013**, *4*, 4505−4511.
(17) Huang, W.; Jiang, Y.; Li, X.; Li, X.; Wang, J.; Wu, Q.; Liu, X. Solvothermal Synthesis of Microporous, Crystalline Covalent Organic Framework Nanofibers and Their Colorimetric Nanohybrid Structures. *ACS Appl. Mater. Interfaces* **2013**, *5*, 8845−8849.
(18) Ding, X.; Feng, X.; Saeki, A.; Seki, S.; Nagai, A.; Jiang, D. Conducting Metallophthalocyanine 2D Covalent Organic Frameworks: The Role of Central Metals in Controlling π-Electronic Functions. *Chem. Commun.* **2012**, *48*, 8952−8954.
(19) Wan, S.; Guo, J.; Kim, J.; Ihee, H.; Jiang, D. A Belt-Shaped, Blue Luminescent, and Semiconducting Covalent Organic Framework. *Angew. Chem., Int. Ed.* **2008**, *47*, 8826−8830.
(20) Dalapati, S.; Jin, S.; Gao, J.; Xu, Y.; Nagai, A.; Jiang, D. An Azine-Linked Covalent Organic Framework. *J. Am. Chem. Soc.* **2013**, *135*, 17310−17313.
(21) Feng, X.; Ding, X.; Jiang, D. Covalent Organic Frameworks. *Chem. Soc. Rev.* **2012**, *41*, 6010−6022.
(22) Feng, X.; Liu, L.; Honsho, Y.; Saeki, A.; Seki, S.; Irle, S.; Dong, Y.; Nagai, A.; Jiang, D. High-Rate Charge-Carrier Transport in

DOI: 10.1021/acs.chemmater.5b02358
Chem. Mater. 2015, 27, 5487−5490

Porphyrin Covalent Organic Frameworks: Switching from Hole to Electron to Ambipolar Conduction. *Angew. Chem., Int. Ed.* **2012**, *51*, 2618−2622.
(23) Zhang, Y. B.; Su, J.; Furukawa, H.; Yun, Y.; Gándara, F.; Duong, A.; Zou, X.; Yaghi, O. M. Single-Crystal Structure of a Covalent Organic Framework. *J. Am. Chem. Soc.* **2013**, *135*, 16336−16339.
(24) Côté, A. P.; El-Kaderi, H. M.; Furukawa, H.; Hunt, J. R.; Yaghi, O. M. Reticular Synthesis of Microporous and Mesoporous 2D Covalent Organic Frameworks. *J. Am. Chem. Soc.* **2007**, *129*, 12914−12915.
(25) Wan, S.; Gándara, F.; Asano, A.; Furukawa, H.; Saeki, A.; Dey, S. K.; Liao, L.; Ambrogio, M. W.; Botros, Y. Y.; Duan, X.; et al. Covalent Organic Frameworks with High Charge Carrier Mobility. *Chem. Mater.* **2011**, *23*, 4094−4097.
(26) El-Kaderi, H. M.; Hunt, J. R.; Mendoza-Cortés, J. L.; Côté, A. P.; Taylor, R. E.; O'Keeffe, M.; Yaghi, O. M. Designed Synthesis of 3D Covalent Organic Frameworks. *Science* **2007**, *316*, 268−272.
(27) Côté, A. P.; Benin, A. I.; Ockwig, N. W.; O'Keeffe, M.; Matzger, A. J.; Yaghi, O. M. Porous, Crystalline, Covalent Organic Frameworks. *Science* **2005**, *310*, 1166−1170.
(28) Ding, S.-Y.; Wang, W. Covalent Organic Frameworks (COFs): From Design to Applications. *Chem. Soc. Rev.* **2013**, *42*, 548−568.
(29) Kataoka, Y.; Sato, K.; Miyazaki, Y.; Masuda, K.; Tanaka, H.; Naito, S.; Mori, W. Photocatalytic Hydrogen Production from Water Using Porous Material $[Ru_2(p\text{-}BDC)_2]_n$. *Energy Environ. Sci.* **2009**, *2*, 397−400.
(30) Kent, C. A.; Mehl, B. P.; Ma, L.; Papanikolas, J. M.; Meyer, T. J.; Lin, W. Energy Transfer Dynamics in Metal-Organic Frameworks. *J. Am. Chem. Soc.* **2010**, *132*, 12767−12769.
(31) Narayan, T. C.; Miyakai, T.; Seki, S.; Dincă, M. High Charge Mobility in a Tetrathiafulvalene-Based Microporous Metal-Organic Framework. *J. Am. Chem. Soc.* **2012**, *134*, 12932−12935.
(32) Sheberla, D.; Sun, L.; Blood-Forsythe, M. A.; Er, S.; Wade, C. R.; Brozek, C. K.; Aspuru-Guzik, A.; Dincă, M. High Electrical Conductivity in Ni_3(2,3,6,7,10,11-hexaiminotriphenylene)$_2$, a Semiconducting Metal-Organic Graphene Analogue. *J. Am. Chem. Soc.* **2014**, *136*, 8859−8862.
(33) Bertrand, G. H. V.; Michaelis, V. K.; Ong, T.-C.; Griffin, R. G.; Dincă, M. Thiophene-Based Covalent Organic Frameworks. *Proc. Natl. Acad. Sci. U. S. A.* **2013**, *110*, 4923−4928.
(34) Dogru, M.; Handloser, M.; Auras, F.; Kunz, T.; Medina, D.; Hartschuh, A.; Knochel, P.; Bein, T. A Photoconductive Thienothiophene-Based Covalent Organic Framework Showing Charge Transfer towards Included Fullerene. *Angew. Chem., Int. Ed.* **2013**, *52*, 2920−2924.
(35) Medina, D. D.; Werner, V.; Auras, F.; Tautz, R.; Dogru, M.; Schuster, J.; Linke, S.; Döblinger, M.; Feldmann, J.; Knochel, P.; et al. Oriented Thin Films of a Benzodithiophene Covalent Organic Framework. *ACS Nano* **2014**, *8*, 4042−4052.
(36) Jin, S.; Sakurai, T.; Kowalczyk, T.; Dalapati, S.; Xu, F.; Wei, H.; Chen, X.; Gao, J.; Seki, S.; Irle, S.; et al. Two-Dimensional Tetrathiafulvalene Covalent Organic Frameworks: Towards Latticed Conductive Organic Salts. *Chem. - Eur. J.* **2014**, *20*, 14608−14613.
(37) Cai, S.; Zhang, Y.; Pun, A. B.; He, B.; Yang, J.; Toma, F.; Sharp, I. D.; Yaghi, O.; Fan, J.; Zheng, S.; et al. Tunable Electrical Conductivity in Oriented Thin Films of Tetrathiafulvalene-Based Covalent Organic Framework. *Chem. Sci.* **2014**, *5*, 4693−4700.
(38) Ding, H.; Li, Y.; Hu, H.; Sun, Y.; Wang, J.; Wang, C.; Wang, C.; Zhang, G.; Wang, B.; Xu, W.; Zhang, D. A Tetrathiafulvalene-Based Electroactive Covalent Organic Framework. *Chem. - Eur. J.* **2014**, *20*, 14614−14618.
(39) Patra, A.; Bendikov, M. Selenium- and Tellurium-Containing Organic π-Conjugated Oligomers and Polymers. In *PATAI'S Chemistry of Functional Groups*; Rappoport, Z., Ed.; John Wiley & Sons: Chichester, U.K., 2011.
(40) Liu, X.; He, R.; Shen, W.; Li, M. Theoretical Design of Donor-Acceptor Conjugated Copolymers Based on Furo-, Thieno-, and Selenopheno[3,4-c]thiophene-4,6-dione and Benzodithiophene Units for Organic Solar Cells. *J. Mol. Model.* **2013**, *19*, 4283−4291.
(41) Keshtov, M. L.; Sharma, G. D.; Kochurov, V. S.; Khokhlov, A. R. New Donor−acceptor Conjugated Polymers Based on benzo[1,2-b:4,5-b′]dithiophene for Photovoltaic Cells. *Synth. Met.* **2013**, *166*, 7−13.
(42) Byun, Y.-S.; Kim, J.-H.; Park, J. B.; Kang, I.-N.; Jin, S.-H.; Hwang, D.-H. Full Donor-Type Conjugated Polymers Consisting of Alkoxy- or Alkylselenophene-Substituted Benzodithiophene and Thiophene Units for Organic Photovoltaic Devices. *Synth. Met.* **2013**, *168*, 23−30.
(43) Wen, S.; Dong, Q.; Cheng, W.; Li, P.; Xu, B.; Tian, W. A Benzo[1,2-b:4,5-b′]dithiophene-Based Copolymer with Deep HOMO Level for Efficient Polymer Solar Cells. *Sol. Energy Mater. Sol. Cells* **2012**, *100*, 239−245.
(44) Jahnke, A. A.; Seferos, D. S. Polytellurophenes. *Macromol. Rapid Commun.* **2011**, *32*, 943−951.
(45) Jahnke, A. A.; Howe, G. W.; Seferos, D. S. Polytellurophenes with Properties Controlled by Tellurium-Coordination. *Angew. Chem., Int. Ed.* **2010**, *49*, 10140−10144.
(46) Gao, P.; Beckmann, D.; Tsao, H. N.; Feng, X.; Enkelmann, V.; Pisula, W.; Müllen, K. Benzo[1,2-b:4,5-b′]bis[*b*]benzothiophene as Solution Processible Organic Semiconductor for Field-Effect Transistors. *Chem. Commun.* **2008**, 1548−1550.
(47) Birkmire, R. W.; McCandless, B. E. CdTe Thin Film Technology: Leading Thin Film PV into the Future. *Curr. Opin. Solid State Mater. Sci.* **2010**, *14*, 139−142.
(48) Ramamoorthy, K.; Kumar, K.; Chandramohan, R.; Sankaranarayanan, K. Review on Material Properties of IZO Thin Films Useful as Epi-N-TCOs in Opto-Electronic (SIS Solar Cells, Polymeric LEDs) Devices. *Mater. Sci. Eng., B* **2006**, *126*, 1−15.
(49) Heeney, M.; Zhang, W.; Crouch, D. J.; Chabinyc, M. L.; Gordeyev, S.; Hamilton, R.; Higgins, S. J.; McCulloch, I.; Skabara, P. J.; Sparrowe, D.; et al. Regioregular Poly(3-hexyl)selenophene: A Low Band Gap Organic Hole Transporting Polymer. *Chem. Commun.* **2007**, 5061−5063.
(50) Patra, A.; Wijsboom, Y. H.; Zade, S. S.; Li, M.; Sheynin, Y.; Leitus, G.; Bendikov, M. Poly(3,4-ethylenedioxyselenophene). *J. Am. Chem. Soc.* **2008**, *130*, 6734−6736.
(51) Patra, A.; Bendikov, M. Polyselenophenes. *J. Mater. Chem.* **2010**, *20*, 422−433.
(52) Cortizo-Lacalle, D.; Skabara, P. J.; Westgate, T. D. *Handbook of Chalcogen Chemistry*; Devillanova, F., du Mont, W.-W., Eds.; Royal Society of Chemistry: Cambridge, U.K., 2013.
(53) Takimiya, K.; Konda, Y.; Ebata, H.; Niihara, N.; Otsubo, T. Facile Synthesis, Structure, and Properties of benzo[1,2-b: 4,5-b′]dichalcogenophenes. *J. Org. Chem.* **2005**, *70*, 10569−10571.
(54) *Boronic Acids*, 2nd ed.; Hall, D. G., Ed.; Wiley−VCH: Weinheim, Germany, 2011.
(55) Feldblyum, J. I.; Liu, M.; Gidley, D. W.; Matzger, A. J. Reconciling the Discrepancies between Crystallographic Porosity and Guest Access as Exemplified by Zn-HKUST-1. *J. Am. Chem. Soc.* **2011**, *133*, 18257−18263.

DOI: 10.1021/acs.chemmater.5b02358
Chem. Mater. 2015, 27, 5487−5490